STM JOURNALS

Recent Trends in
Fluid Mechanics

ISSN: 2455-1961
Volume 12, Issue 3, 2025
September–December
DOI (Journal): 10.37591/RTFM

https://journals.stmjournals.com/rtfm

Research RTFM

Optimizing Heat Dissipation: Analysis of Air-Cooled Fins for Electronic Equipment

Sharmishta Menon[1], Naveen Solanki[2,*]

Abstract

This paper focuses on the thermal management of electronic components in modern technologies like RADAR electronics, UAV and Drone technologies, Automotive Electronic Components, etc. The main objective of this research is to design and develop an efficient heat dissipation system, using fins, for an electronic component with dimensions of 80 x 300 mm, dissipating 30W heat. The process starts by calculating essential parameters for fin design, followed by modeling the fins in SOLIDWORKS using the computed dimensions. SOLIDWORKS, a leading Computer-Aided Design (CAD) software, enables precise 3D modeling, ensuring the fins meet design specifications accurately. This approach integrates analytical calculations with advanced CAD modeling for efficient and reliable fin development. After designing, the analysis of the model is done using Ansys Fluent software student version, a leading tool in Finite Element Analysis (FEA). The paper delves into the theoretical background of fin calculation and aims to optimize fin design, maximizing heat transfer efficiency while minimizing the material wastage by reducing surface area and finding optimum fin height. The analysis results can validate the findings derived from theoretical calculations.

Keywords: Optimizing heat dissipation, air cooled fins, CFD analysis, Solidworks, Ansys

INTRODUCTION

Efficient thermal management is a critical challenge for the electronics industry. As electronic components continue to shrink and power consumption increases, the need for effective cooling solutions has become increasingly important. Overheating can lead to performance degradation, system failure, and reduced component lifespans. This study aims to contribute to the development of a more efficient and effective cooling system by analyzing the performance of an air-cooled system under various control conditions.

A heat dissipation structure (fins) is designed for the electronic part that can effectively remove the generated heat under the given conditions. The fins should be able to maintain the temperature of the part within acceptable limits to ensure reliable operation and to prevent damage.

***Author for Correspondence**
Naveen Solanki
E-mail: naveensolanki@mait.ac.in

[1]Student, Department of Mechanical Engineering, Maharaja Agrasen Institute of Technology, Delhi, Rohini Sec-22, India
[2]Assistant Professor, Department of Mechanical Engineering, Maharaja Agrasen Institute of Technology, Delhi, Rohini Sec-22, India

Received Date: August 13, 2025
Accepted Date: August 23, 2025
Published Date: October 08, 2025

Citation: Sharmishta Menon, Naveen Solanki. Optimizing Heat Dissipation: Analysis of Air-Cooled Fins for Electronic Equipment. Recent Trends in Fluid Mechanics. 2025; 12(3): 26–50p.

The optimization and enhancement of heat transfer systems have been areas of significant research interest. Various studies have explored different geometries, materials, and numerical methods to improve thermal performance and system efficiency. Chang-Woo Han and Seung-Boong Jeong [1] investigated the thermal performance of air-cooled heat sinks with different fin geometries. Because of their greater surface area and better airflow dynamics, they discovered that perforated fins significantly improved heat dissipation. Their experimentally confirmed numerical models had a 5.6% margin of error in the

predicted accuracy. Ahmet Numan Özakin [2] In this study, forced air cooling for solar panels with aluminum fins was examined.

Fins increased thermal efficiency by up to 70% and exergy efficiency by up to 48%, while lowering surface temperature by 10 to 15 °C. Frequent and sparse fins improved cooling by facilitating faster and even airflow between fins and close to the inlets and outputs. Hasan and Bukht Majmader [3] examined entropy generation and thermal enhancement in air-cooled 3D radiators. They increased the rate of heat transmission by up to 134% and significantly decreased the formation of entropy by altering the fin shapes (such as spike-rib or wavy) and adding perforations. Their findings highlight how crucial fin geometry and perforation are to heat exchange performance optimization. Zheng Lan [4] This study used simulations, tests, and a GA-BP neural network to examine the hydraulic and thermal performance of rectangular fin heat sinks under forced convection. The GA-BP model achieves high prediction accuracy, saves resources, and optimizes heat sink design. The results show correlations between the Reynolds number, fin shape, Nusselt number, and friction factor. A multi-scaling investigation of turbulent boundary layers over an isothermally heated flat plate with zero pressure gradient was carried out by Md. Shahneoug Shuvo et al. [5]. They showed that they could accurately estimate turbulent heat transfer properties across a range of Reynolds and Prandtl numbers using sophisticated turbulence models such as Spalart-Allmaras. Their research emphasized the importance of the intermediate scaling layer in turbulent heat transfer systems, and Praharsh Pai Raikar [6] used the adjoint method in conjunction with CFD-based design optimization to enhance the heat exchanger performance. The study optimized tube forms to minimize the pressure drop while preserving heat transmission using CAD parametrization and a RANS solver. According to the results, the thermo-hydraulic performance improved by 19% for identical tubes and 25% for non-similar forms [7].

This study combines numerical techniques and empirical equations to produce a CFD-based thermal model for a fan-cooled plate-fin heat sink. It employed a finite difference approach in MATLAB to estimate the fluid temperature and compute the heat transfer coefficients. Rapid thermal performance prediction and system optimization are facilitated by the model's 10% error margin and speed when compared to CFD simulations. Zhou [8] used numerical simulations to examine supercritical CO_2 heat transport in both uniform and non-uniform cooling scenarios. The distribution of the heat flux along the finned tube was found to be unequal, and it increased with the wind speed. At higher temperatures, the heat transfer coefficient increased by 6.84% due to non-uniform cooling, demonstrating the significance of buoyancy effects and thermophysical characteristics. Zhonghua Zhao [9] In order to decrease overheating and increase efficiency, this study investigated the application of heat dissipation fins in a PV/T system. By altering the fin count (0, 5, and 10) and solar radiation (200–600 W/m^2), it was demonstrated that more fins improve the thermal performance, leading to a significant increase in the photothermal conversion efficiency. Gamal Refai-Ahmed [10] CFD simulations in ANSYS Icepak were utilized in this study to optimize the design of an air-cooled heat sink for high-power electronics. The thermal performance was examined, and the shape of the heat sink was optimized to reduce the temperature and pressure drops. According to these findings, air cooling for 1U or 4U servers might manage up to 55 W/cm².

These studies collectively emphasize the role of innovative geometrical modifications and advanced numerical methods in enhancing the thermal performance of heat exchangers and other cooling systems.

OBJECTIVES AND ASSUMPTIONS

To design and compare the thermal performance of air-cooled fins (heat sinks) under different conditions for electronic equipment with dimensions of (80 mm × 300 mm). This study aims to determine the optimal cooling condition, heat transfer efficiency, fin effectiveness, and potential for cost minimization by reducing material waste.

For the purposes of this analysis, we will assume the following values:

- Electronic Equipment Dimension= 80x300mm
- Heat generated: Q_{gen} for air cooled fins = 30W
- T (junction)= 70˚C
- Fin Material = Aluminum 6061-T6
- Thermal conductivity K(Al) = 167W/m K
- $T_{(outlet)}$- $T_{(inlet)}$= 10˚C
- C_p(air)= 1.005KJ/Kg K
- Density (air)=1.2Kg/m^3
- Internal Resistance= 0.03˚C/W
- Contact Resistance = 0.01˚C/W

There are many electronic components within the 80 × 300 mm dimension that dissipate approximately 30 W of heat, which require thermal management, such as industrial PLCs, HMI panels, IoT devices, Radar Electronics, UAV Technology PDBs.

Aluminum 6061-T6 and 6061-T651 are popular alloys known for their excellent balance of strength, workability, and corrosion resistance. They are widely used in various industries owing to their versatility and ease of manufacture. They are considered economical choices within the aluminum family[11].

METHODOLOGY

The methodology involves a systematic approach to determine the number of fins required to effectively dissipate the generated heat.

A comprehensive analysis was conducted using Excel-based calculations to evaluate the thermal performance of air-cooled fins. The following steps were followed (flowchart in Figure 1):

Step 1: To Find the mass flow rate required for cooling the electronic component of a given Q(gen) as described by Eq. (1).

$$\dot{Q}_{gen} = m\ Cp\ (T_{(outlet)} - T_{\infty}) \tag{1}$$

$$\dot{V}_{(flow\ rate)} = \frac{m(flow\ rate)}{\rho} \tag{2}$$

To find the velocity of flow, we use Eq. (3).

$$V_{(flow\ rate)} = Area \times velocity \tag{3}$$

In both cases, Q_{gen} will be different, considering the heat capacity of both fluids.

Step 2: To determine the Reynolds number to predict the flow pattern, we use Eq. (4). It is crucial to determine whether the flow is laminar or turbulent.

$$R_e = \frac{\rho * U * D_h}{\mu} \tag{4}$$

Step 3: To determine the Nusselt number, the ratio of the total heat transfer (convection + conduction) to the pure conduction heat transfer across a boundary using Eq. (5).

$$N_u = \frac{h * D_h}{k} \tag{5}.$$

For a laminar flow over a flat plate, the Nusselt number can be determined using the following correlation Eq. (6):

$$Nu = 0.664\, Re^{0.5}\, Pr^{1/3} \tag{6}$$

For a turbulent flow over a flat plate, the most commonly used correlation is the Dittus-Boelter equation (Eq. (7):

$$Nu = 0.023 Re^{0.8}\, Pr^{n} \tag{7}$$

Where n=0.3 for cooling.

The convection heat transfer coefficient(h) can be determined by equating the formulas of Nuin equations (6) and (7) [12, 13].

Step 4: To determine the surface temperature that can be attained, we used the general heat transfer equation in Eq. (8):

$$\dot{Q}_{gen} = h\, A(T_s - T_\infty) \tag{8}$$

Step 5: The thermal resistances of the fins and the junction-to-ambient path were calculated. The temperature distribution within the fins and electronic device was estimated using the provided internal and contact resistance using a temperature analogous to the voltage equations in Eq. (9).

From the given internal resistance (R_i) and contact resistance (R_c) of the electronic component in Table 1, we find the temperature loss in that region (temperature absorbed by the electronic component and the component adhesive) using Eq. (9).

$$\dot{Q}_{gen} = \frac{\Delta T}{R} \frac{(Change\ in\ Temp)}{(Resistance)} \tag{9}$$

From the surface temperature, we estimated the junction temperature that could be reached. The estimated Junction Temperature can be derived from Eq. (10):

$$T_{j'} = T_s + (T_j - T_c) + (T_c - T_s) \tag{10}$$

Step 6: By comparing the given junction temp and the estimated junction temp, we can determine whether the fin design is safe using Table 2.

Table 1. Internal and contact resistance with temperature loss.

Resistance	Value	Temp loss (Tj-Tc)
Internal resistance	0.03˚C/W	0.9˚C
Contact resistance	0.01˚C/W	0.3˚C

Table 2. Comparison table.

Cases	Remarks
$T_{j'}$(estimated) < T_j(given)	The designed fin is safe and efficient
$T_{j'}$(estimated) > T_j (given)	Need to redesign fins as its surface is reaching a temperature greater than the max temp the electronic component can attain

Step 7: To find heat transfer through the fins.

For a short fin without an insulated tip, the temperature distribution along the fin and the heat transfer through the fin can be expressed by Eq. (11) (corrected length **(Lc)**):

$$Q_{gen} = \sqrt{hPkA} * \theta_{b^*} \tan h(mL_C) \quad (11)$$

$$Q_{\text{total}} = Q_{(\text{fins})} + Q_{(\text{non fin area})} \quad (12)$$

Step 8: The heat transfer efficiency and fin effectiveness are calculated to assess the performance of the cooling solution.

THE ANALYSIS MODEL USED FOR THIS PAPER

To analyze the thermal performance of electronic components under various conditions, such as the number of fins, different velocities, and temperatures, there is a need to perform calculations in a systematic order, which can provide a structured approach to breaking down the problem into smaller, manageable components.

The tree diagram shows that the analysis considers the thermal performance of the system under different combinations of the numbers of fins N1 and N2, velocities V1 and V2, and temperatures T1 and T2. This allows for a comprehensive evaluation of how the behavior of the system changes under different conditions, as shown in Figure 2.

Here, the analysis is done by using the combinations:

Number of fins

- N1= 30fins
- N2= 20fins
- N3= 10fins

Velocities

- V1= 103.64m/sec
- V2= 90m/sec
- V3= 60m/sec
- V4= 30m/sec
- V5= 10m/sec
- V6= 2m/sec
- V7= 1m/sec
- V8= 0.5m/sec (room air velocity)

Temperatures

- T1= 20°C (room temp)
- T2= 55°C (extreme dry desert conditions)
- T3= (-10)°C (freezing temp)

Through this tree diagram approach, we can systematically analyze the thermal performance of the dummy electronic component (as mentioned in the paper's objective and assumptions section) and identify potential improvements by comparing the results to ensure reliable and efficient operation under various conditions.

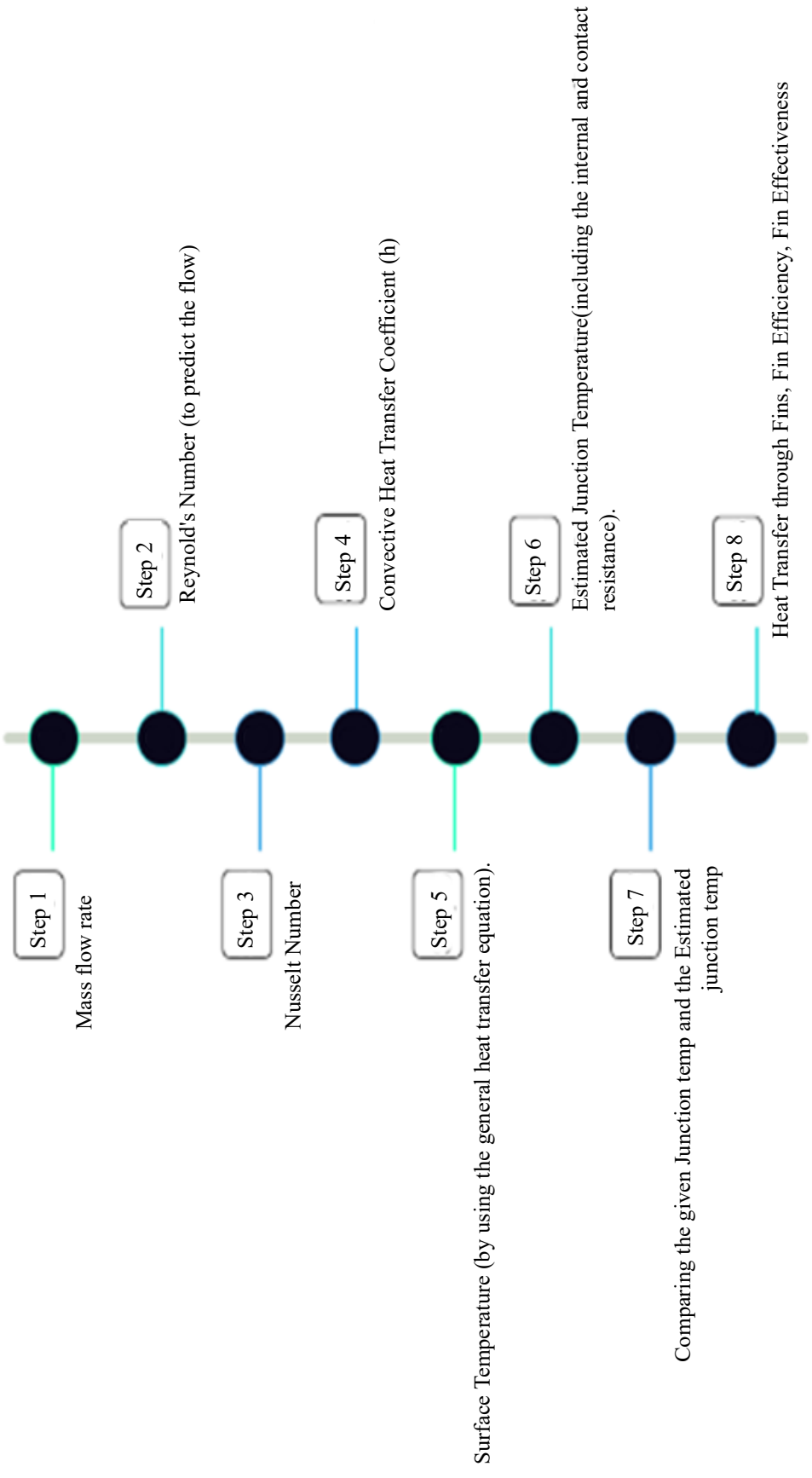

Figure 1. Methodology flow chart.

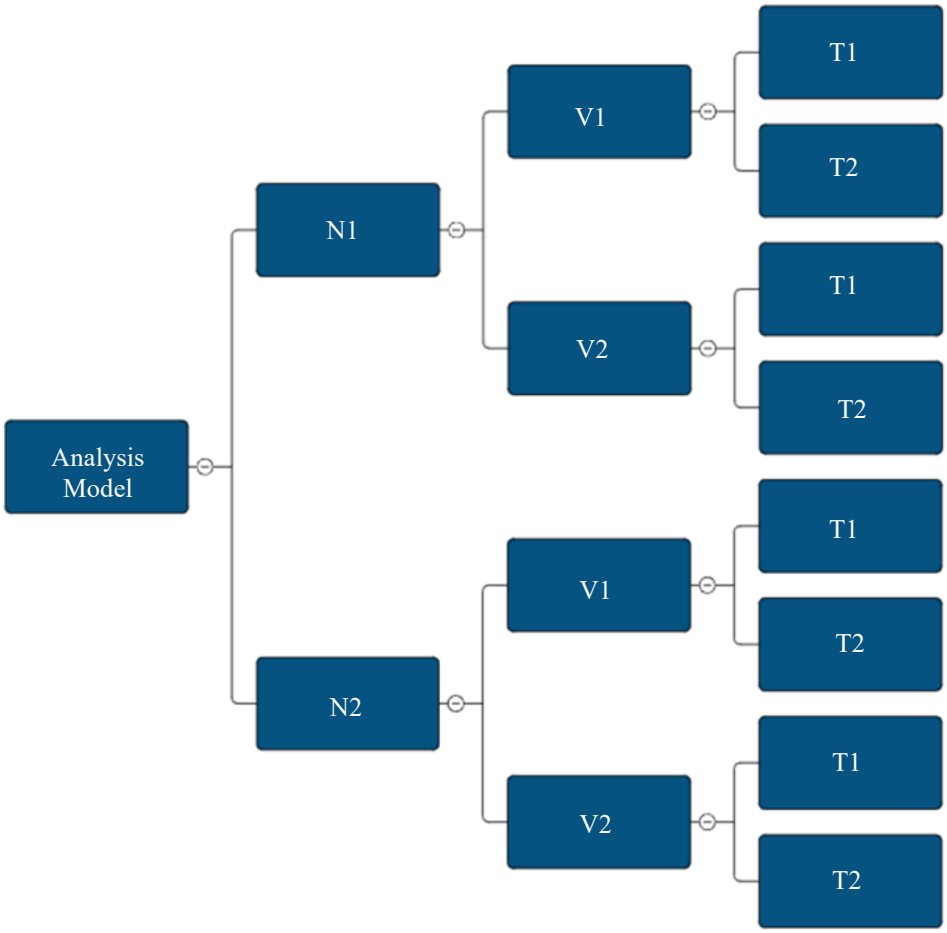

Figure 2. Analysis Model.

RESULTS AND DISCUSSIONS

These are the optimal fin heights determined for various velocities considering the surrounding temperature.

The calculations in the table in Figure 3 can be represented graphically, which provides a visual representation of the thermal performance of air-cooled fins under different conditions. The graphs were used to analyze trends, identify optimal parameters, and visualize the impact of various factors on the behavior of the system.

Case 1

At T=20 °C, the optimum fin height at various velocities is represented by the graph in Figure 4, and the maximum heat transfer at various velocities is represented by the graph in Figure 5.

Case 2

At T=55 °C, the optimum fin height at various velocities is represented by the graph in Figure 6, and the maximum heat transfer at various velocities is represented by the graph in Figure 7.

Case 3

At T= (-10)°C the optimum fin height at various velocities is represented by the graph in Figure 8, and the maximum heat transfer at various velocities is represented by the graph in Figure 9.

Here, the green line represents the 20-fin design, and the blue line represents the 30fins design the green bars represent the 20-fin design and blue bars represent the 30fins design.

no of fins	velocity	temperature	lengthof fin from base	Q(max)	T'j(estimated)
n1=30	103.64	20	0.001	30.01048655	25.02158453
		55	0.001	30.01048655	60.02158453
		(-10)	0.001	30.01048655	5.021584533
	90	20	0.001	30.01394122	25.4783015
		55	0.001	30.01394122	60.4783015
		(-10)	0.001	30.01394122	-4.521698504
	60	20	0.001	30.02195471	27.11758349
		55	0.001	30.02195471	62.11758349
		(-10)	0.001	30.02195471	-2.882416515
	30	20	0.001	30.03086619	31.50311127
		55	0.001	30.03086619	66.50311127
		(-10)	0.001	30.03086619	1.503111273
	10	20	0.002	30.04381228	38.56853627
		55	0.003	30.03502473	69.56040897
		(-10)	0.003	30.04381228	8.568536272
	2	20	0.003	30.05979943	69.6167636
		55	0.014	29.90247697	69.88298973
		(-10)	0.003	30.05979943	39.6167636
	1	20	0.007	30.05621973	65.03519185
		55	0.026	29.72636973	69.56438349
		(-10)	0.004	30.06563786	59.69250499
	0.5	20	0.012	30.04383949	68.90093047
		55	0.045	29.47122399	69.92688365
		(-10)	0.007	30.06804194	67.52150191
n2=20	103.64	20	0.001	30.00811661	25.65850778
		55	0.001	30.00811661	60.65850778
		(-10)	0.001	30.00811661	-4.341492222
	90	20	0.001	30.01080357	26.19134334
		55	0.001	30.01080357	61.19134334
		(-10)	0.001	30.01080357	-3.808656663
	60	20	0.001	30.01703627	28.10383577
		55	0.001	30.01703627	63.10383577
		(-10)	0.001	30.01703627	-1.89616423
	30	20	0.001	30.02396741	33.22027624
		55	0.001	30.02396741	68.22027624
		(-10)	0.001	30.02396741	3.220276237
	10	20	0.002	30.0364805	42.91064469
		55	0.005	29.98935604	68.60608285
		(-10)	0.002	30.0364805	12.91064469
	2	20	0.005	30.04871209	66.15838277
		55	0.021	29.68474219	69.88298623
		(-10)	0.004	30.0521481	43.65144641
	1	20	0.01	30.03042233	66.8616367
		55	0.038	29.33503832	69.89849111
		(-10)	0.005	30.05837475	69.4770909
	0.5	20	0.018	29.99043914	68.90091645
		55	0.068	28.72748916	69.82883333
		(-10)	0.011	30.04773206	64.58602507
n3=10	103.64	(-10)	0.001	30.00481071	-3.449801144
	90	(-10)	0.001	30.00647689	-2.810388944
	60	(-10)	0.001	30.01022246	-0.515396747
	30	(-10)	0.002	30.01160583	3.220256704
	10	(-10)	0.002	30.02427092	20.14747892
	2	(-10)	0.004	30.0391115	69.87717116
	1	(-10)	0.012	34.48947173	69.92100708
	0.5	(-10)	0.021	29.600027	33.60080547

Figure 3. Fin calculation results.

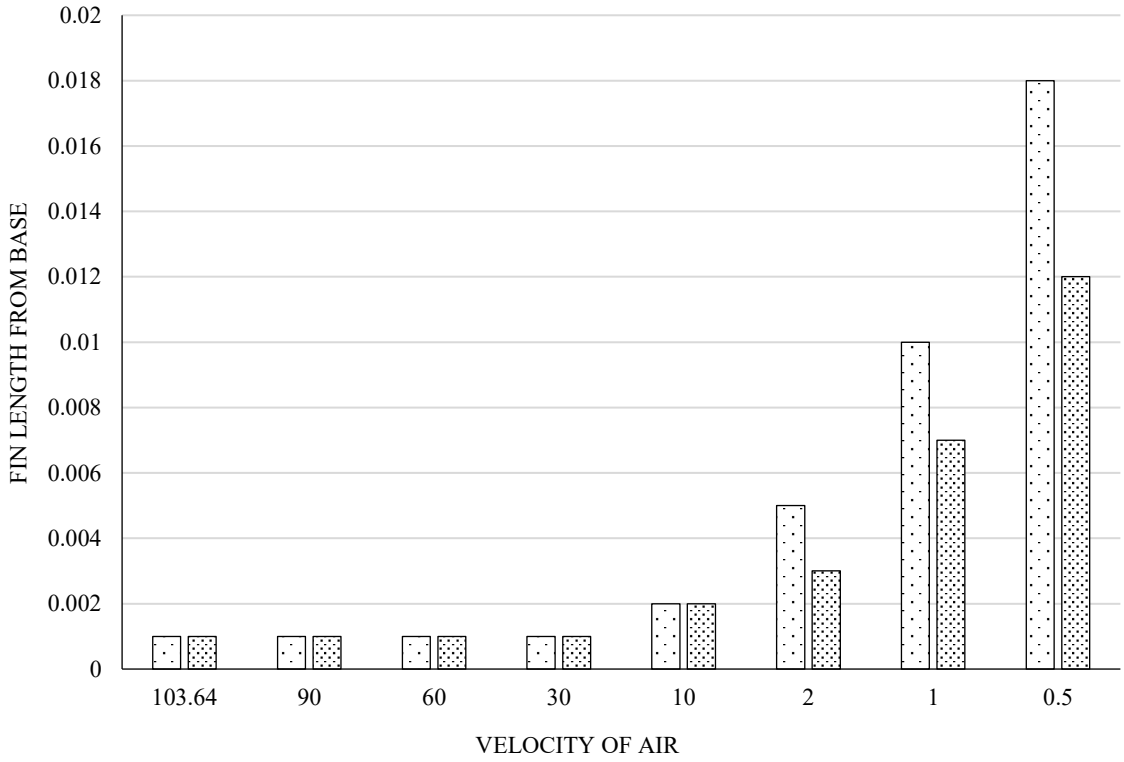

Figure 4. Fin height vs velocity of air at T= 20°C.

The green and blue bars represent the 20fins design and 30fins design.

Here the green line represents the 10-fin design, and the yellow lines represent the 20-fin design and orange line represents 30-fin design.

Here the green line represents the 10-fin design, and the yellow lines represent the 20-fin design and orange line represents 30-fin design.

Observations

- The fin height is inversely proportional to the air velocity for all three cases, as shown in Figures 4, 6, and 8.
- Also derived from the general heat transfer equation, i.e. Eq. (8).
- The fin height became independent of the fin spacing at high velocities, as shown in Figures 4, 6, and 8.
- As the velocity increases, the kinetic energy also increases, leading to a decrease in the Boundary Layer thickness, which in turn decreases the interference between two adjacent fin plates, thereby improving the heat dissipation.
- The fin design is insufficient to effectively dissipate heat at lower velocities owing to the high ambient temperature, as shown in the graph in Figure 7.

Effective heat transfer at higher ambient temperatures can still be achieved owing to the increased fluid velocities, which enhance the heat transfer coefficient, efficient transport of energy, and potential for turbulent flow.

Warmer fluids often have lower viscosities, allowing for better heat exchange.

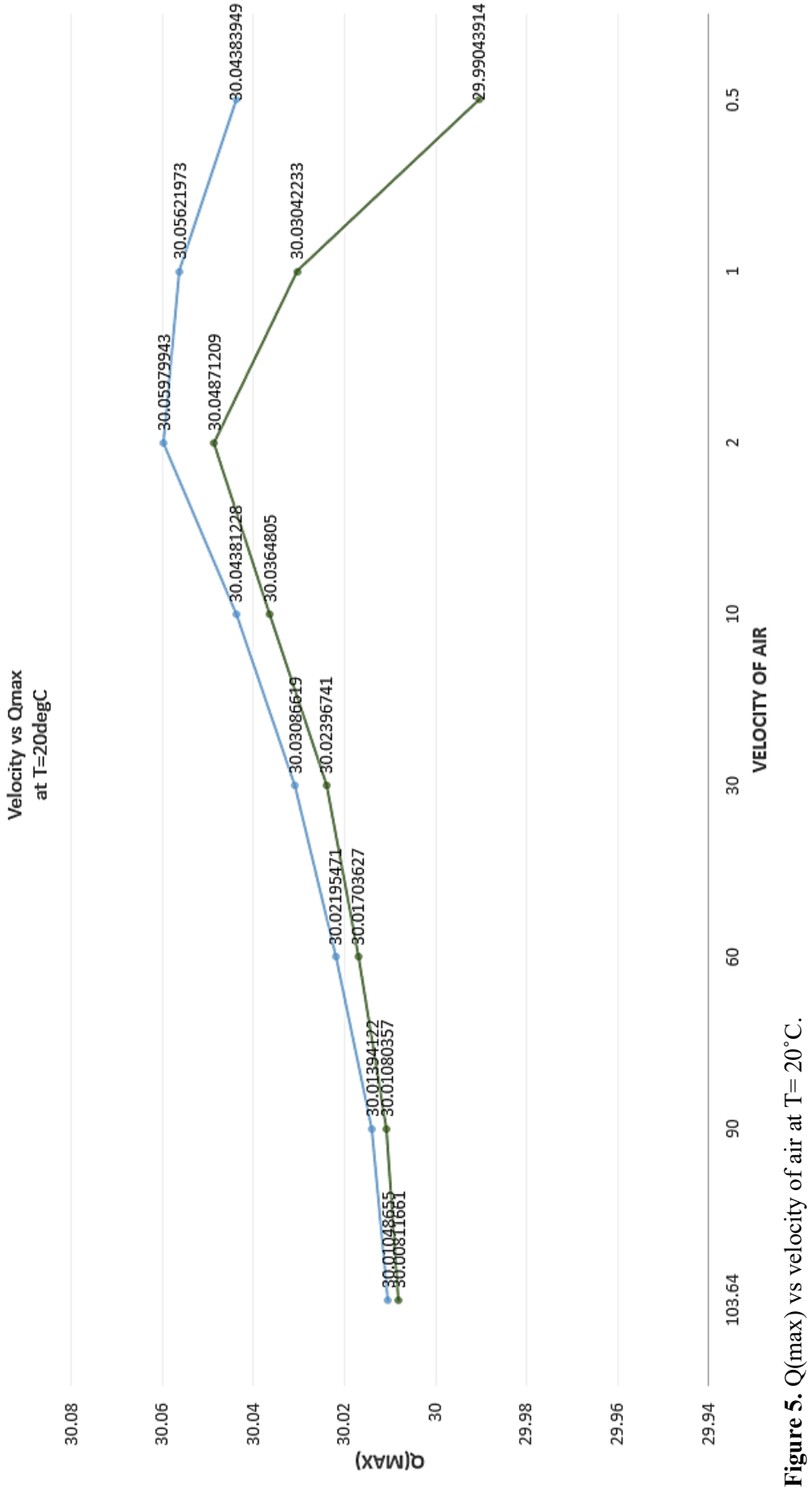

Figure 5. Q(max) vs velocity of air at T= 20˚C.

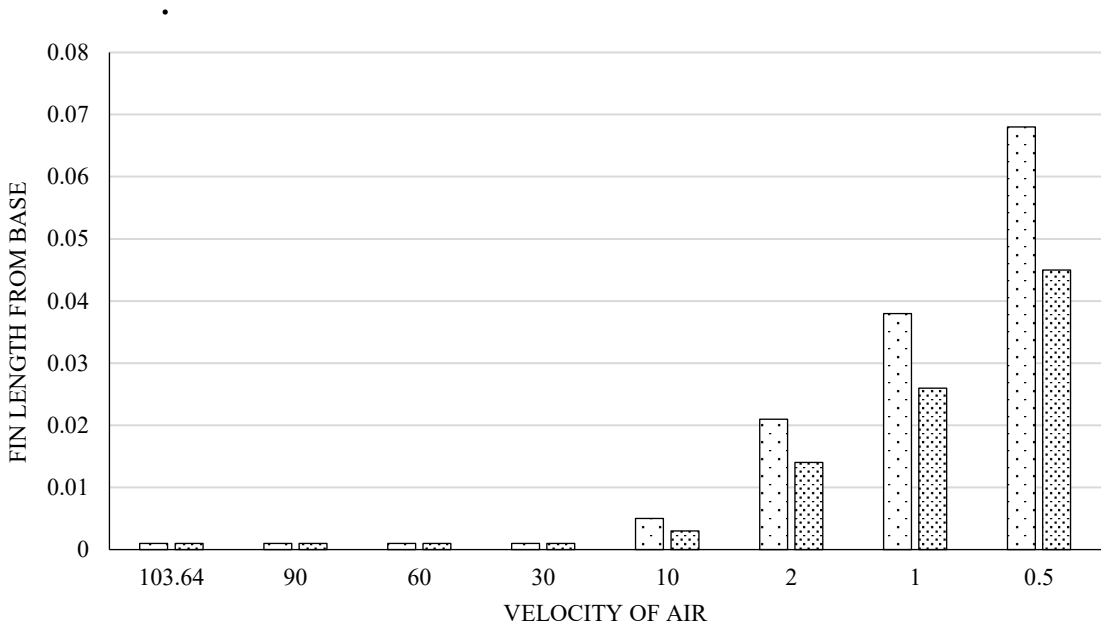

Figure 6. Fin height versus velocity of air at T= 55°C.

Higher fluid velocities (more kinetic energy) can lead to a turbulent flow, which enhances mixing and disrupts the boundary layer. This results in better contact between the fluid and fin surfaces, facilitating more effective heat transfer, even at lower temperature gradients.

In addition, at high velocities, a pressure gradient is created, which causes the boundary layer of the two adjacent fins to overlap, leading to increased interference[14].

1. The boundary Layer thickness decreases with an increase in the kinetic energy, temperature, and free stream velocity. This leads to an increased heat transfer.
2. A specific equilibrium state is observed within a defined velocity range at a given temperature, where the fin height remains the same but the spacing differs; heat dissipation remains constant owing to the interplay between the surface area and boundary layer effect for two different fin designs (no. of fins), as shown in the graph in Figure 8.

Analysis based on Optimum $Q_{(max)}$

The following Figure 10. represents the data of all cases with optimum Q(max), along with the corresponding fin efficiency and effectiveness derived from the graphs.

- In case of T=20°C the optimum Q(max) for different fin arrangement is attained at lower velocities i.e. 2m/sec.
- In case of T=55°C, the optimum Q(max) for different fin arrangements attained at higher velocities i.e. 10-30m/sec.
- In case of T= (-10)°C the optimum Q(max) for different fin arrangements is attained at much lower velocities i.e. 0.5-1 m/sec, as from Figure 10.

At T = (-10)°C, the optimum Q(max) was achieved with a 10-fin arrangement, but the fin effectiveness was relatively low at 0.55. This means that the fins enhance the heat transfer by 55% compared to a surface without fins, indicating moderate effectiveness. While this design balances the heat dissipation and the number of fins, fins with lower effectiveness can create significant thermal gradients, leading to thermal stress. These stresses, combined with frequent heating and cooling cycles, can accelerate fatigue damage and reduce the lifespan of the heat sink. Thus, while the fin arrangement meets short-term heat dissipation requirements, long-term reliability and durability may be compromised, highlighting the need to balance immediate performance with long-term system reliability [15].

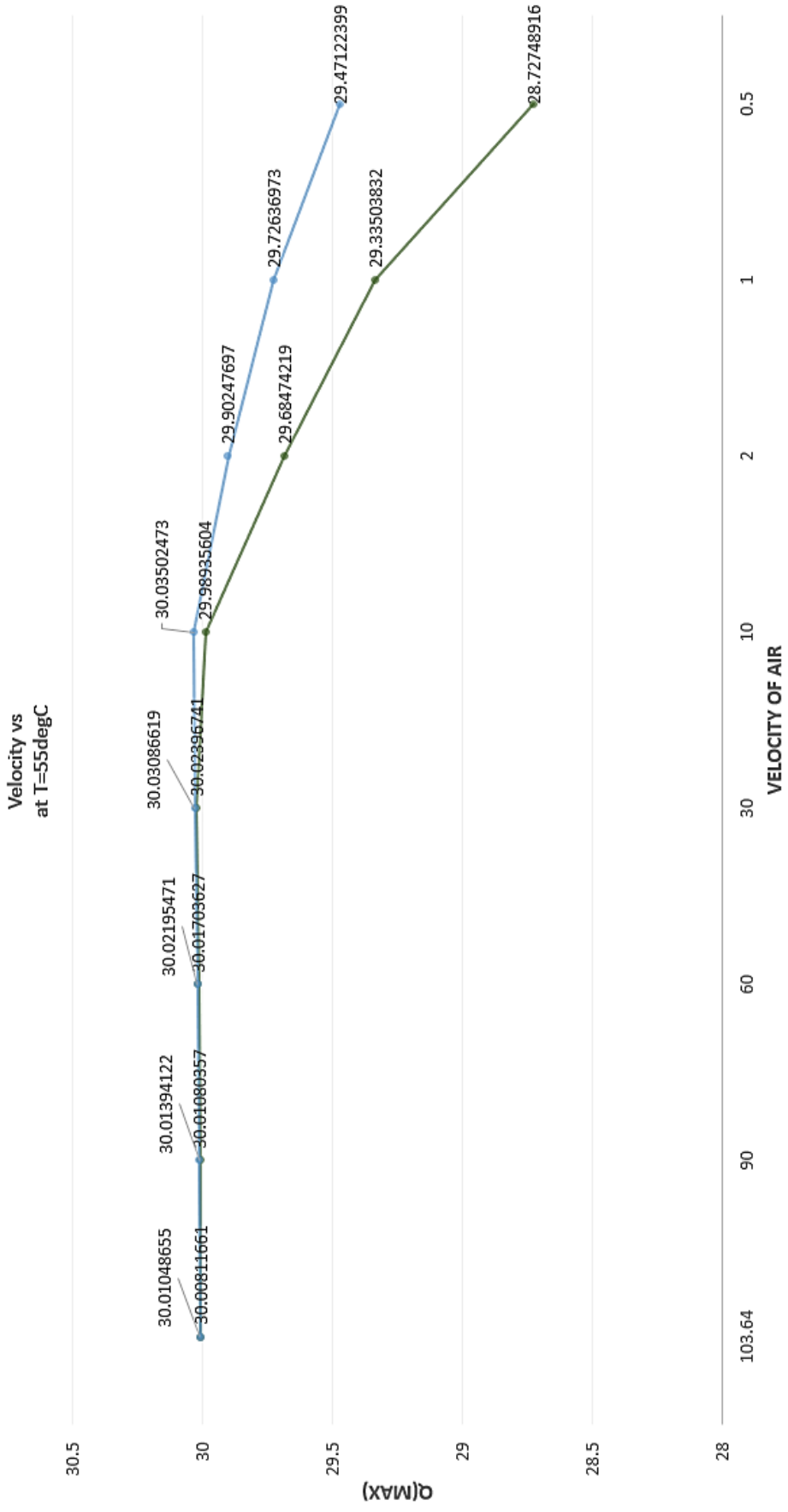

Figure 7. Q(max) versus velocity of air at T= 55°C.

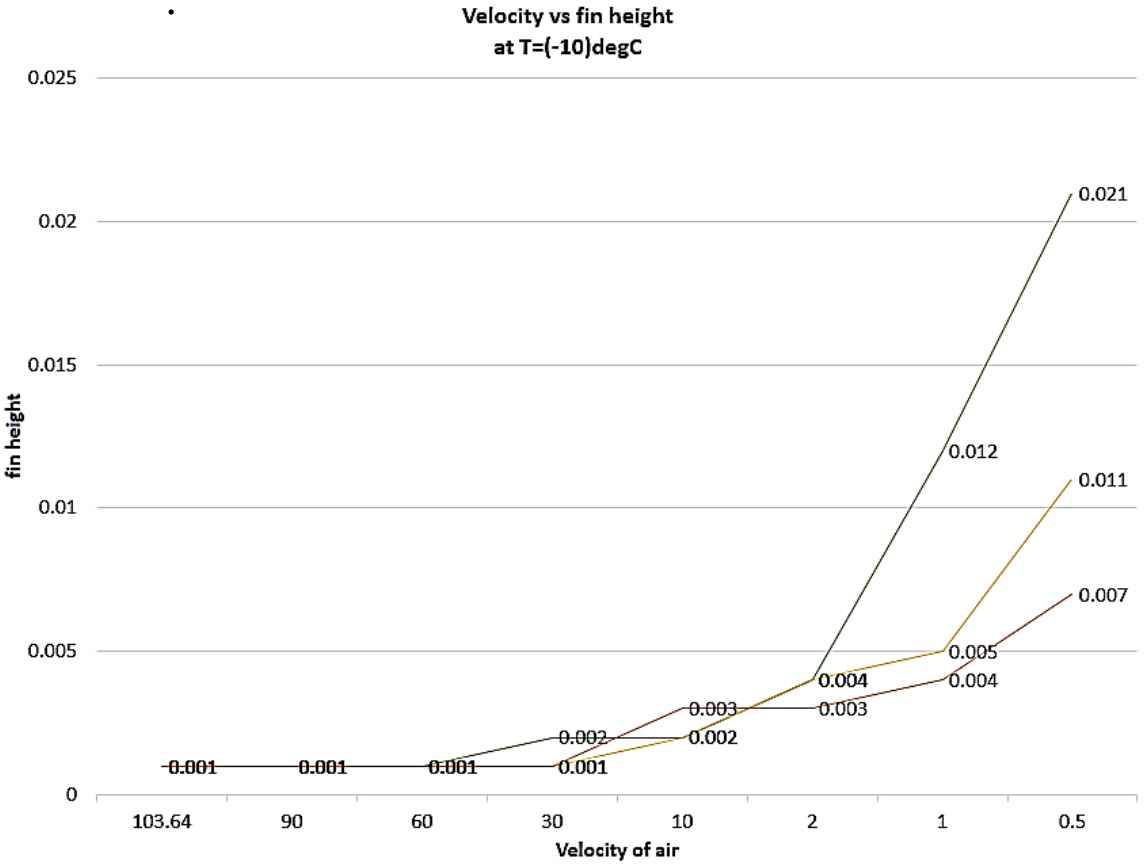

Figure 8. Fin height versus velocity of air at T= (-10)°C.

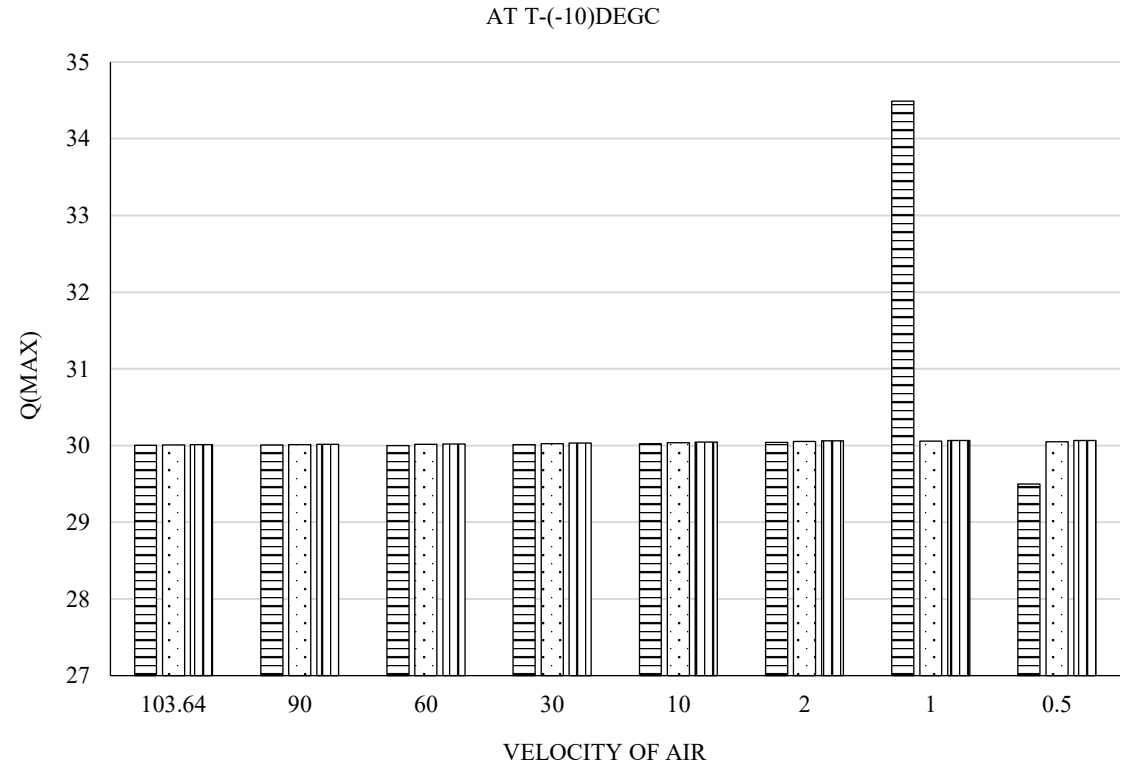

Figure 9. Q(max) versus velocity of air at T= (-10)˚C.

TEMPERATURE (deg C)	NO. OF FINS	VELOCITY (m/sec)	OPTIMUM Q(max) (W)	FIN HEIGHT (m)	FIN EFFICIENCY	FIN EFFECTIVENESS
	30	2	30.05979943	0.003	0.999610785	1.001993403
20	20	2	30.04871209	0.005	0.999039205	1.001625778
	30	10	30.035024	0.003	0.998591251	1.001175363
- 55	20	30	30.02396741	0.001	0.999377073	1.000972092
	10	1	34.48947	0.012	0.997155118	0.552134434
	30	0.5	30.068041	0.007	0.999410283	1.002266163
10	20	1	30.05837475	0.005	0.999447897	1.001947024

Figure 10. Optimum results for each case.

CFD ANALYSIS

Case I – A. Steady State Thermal Analysis for 20 fins.

From the analysis Figure 11, it is confirmed that the surface temperature remains below 70°C, with a maximum value of 55.91°C. This indicates that the finned heat sink design is suitable for application, providing effective thermal management of electronic components.

Table 3. Input values of different parameters for CFD analysis.

Parameters	Input Values
Ambient Temperature ($T_{(ambient)}$)	20°C
Heat Generated ($Q_{(gen)}$)	30 W
Temperature Difference ($T_{(outlet)} - T_{(inlet)}$)	10°C
Number of Fins (N)	20 fins
Air Velocity (v)	2 m/s
Convection Coefficient (h)	7.94 W/m²·°C
Fin Height ($h_{(fin)}$)	0.005 m
Mesh Element Size	0.001m

Case I –B. Steady State Thermal Analysis for 30fins.

From the analysis Figure 12, it was confirmed that the surface temperature remained below 70°C, with a maximum value of 58.199°C. This indicates that the finned heat sink design is suitable for application, providing effective thermal management of electronic components.

Table 4. Input values of different parameters for CFD analysis

Parameters	Input Values
Ambient Temperature ($T_{(ambient)}$)	20°C
Heat Generated ($Q_{(gen)}$)	30 W
Temperature Difference ($T_{(outlet)} - T_{(inlet)}$)	10°C
Number of Fins (N)	30 fins
Air Velocity (v)	2 m/s
Convection Coefficient (h)	7.94 W/m²·°C
Fin Height ($h_{(fin)}$)	0.003 m
Mesh Element Size	0.001m

Case II – A. Steady State Thermal Analysis for 20 fins

From the analysis Figure 13, it was confirmed that the surface temperature remained below 70°C, with a maximum value of 66.943°C. This indicates that the finned heat sink design is suitable for application, providing effective thermal management of electronic components.

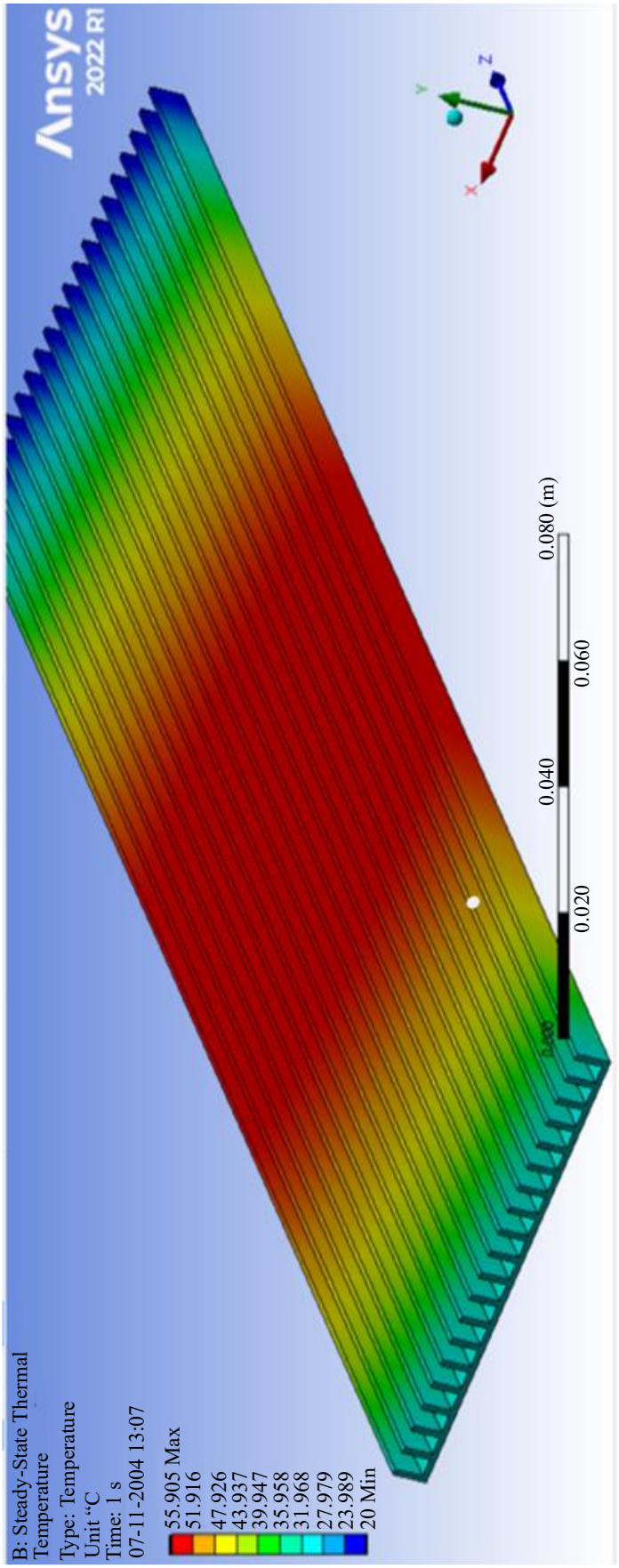

Figure 11. Steady state analysis, temperature variation across surface of fin.

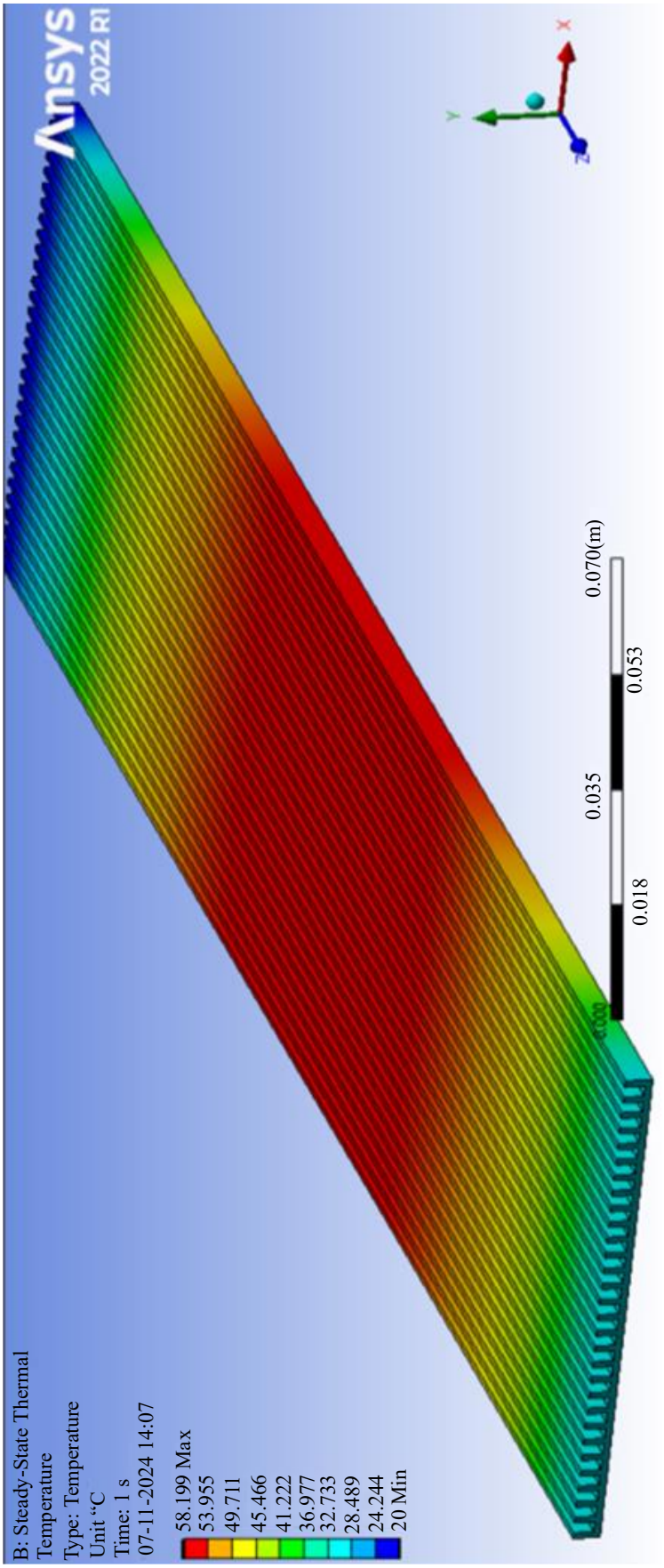

Figure 12. Steady state analysis, temperature variation across surface.

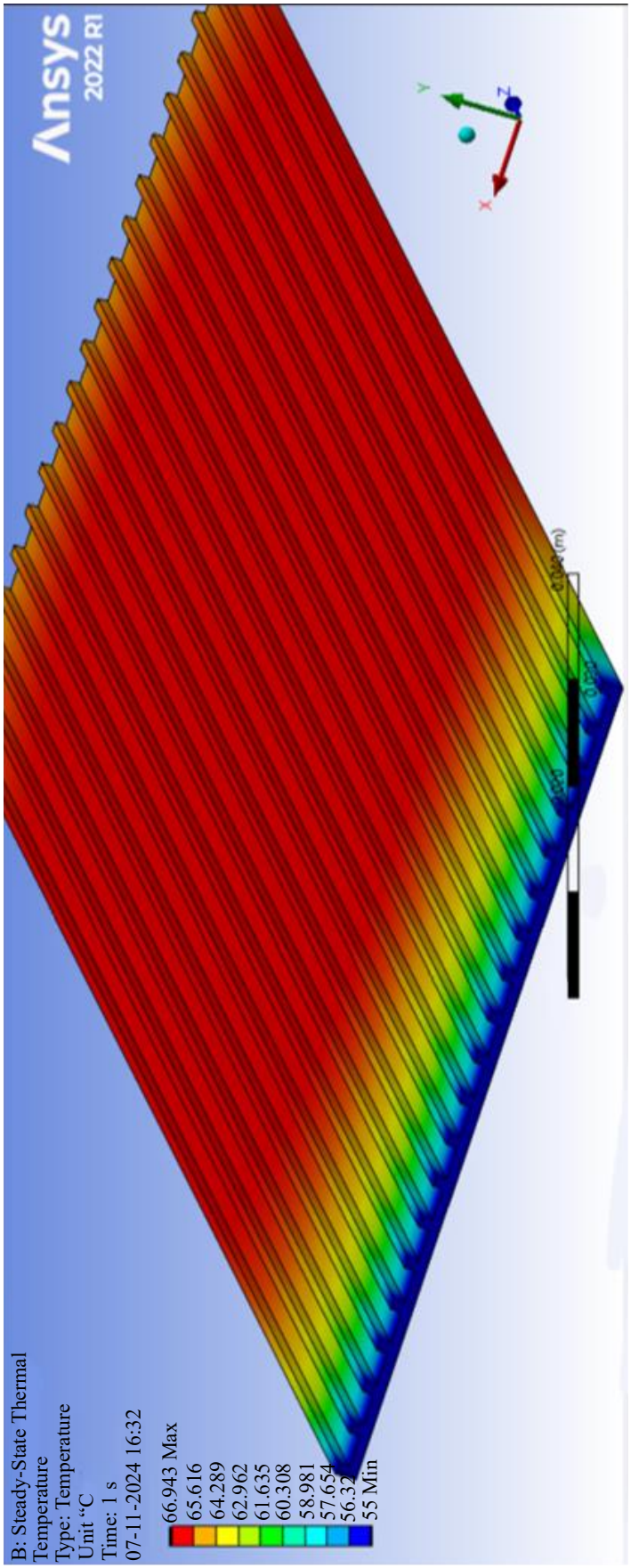

Figure 13. Steady state analysis, temperature variation across surface.

Table 5. Input values of different parameters for CFD analysis.

Parameters	Input Values
Ambient Temperature ($T_{(ambient)}$)	55°C
Heat Generated ($Q_{(gen)}$)	30 W
Temperature Difference ($T_{(outlet)}$– $T_{(inlet)}$)	10°C
Number of Fins (N)	20 fins
Air Velocity (v)	30 m/s
Convection Coefficient (h)	69.327300 W/m²·°C
Fin Height ($h_{(fin)}$)	0.001 m
Mesh Element Size	0.0005m

Case II –B. Steady State Thermal Analysis for 30fins

From the analysis Figure 14, it was confirmed that the surface temperature remained below 70°C, with a maximum value of 68.186°C. This indicates that the finned heat sink design is suitable for application, providing effective thermal management of electronic components.

Table 6. Input values of different parameters for CFD analysis**.**

Parameters	Input Values
Ambient Temperature ($T_{(ambient)}$)	55°C
Heat Generated ($Q_{(gen)}$)	30 W
Temperature Difference ($T_{(outlet)}$ – $T_{(inlet)}$)	10°C
Number of Fins (N)	30 fins
Air Velocity (v)	10 m/s
Convection Coefficient (h)	28.78772092 W/m²·°C
Fin Height ($h_{(fin)}$)	0.003 m
Mesh Element Size	0.001m

Case III – A. Steady State Thermal Analysis for 20 fins

From the analysis Figure 15, it was confirmed that the surface temperature remained below 70°C, with a maximum value of 40.593°C. This indicates that the finned heat sink design is suitable for application, providing effective thermal management of electronic components.

Table 7. Input values of different parameters for CFD analysis

Parameters	Input Values
Ambient Temperature ($T_{(ambient)}$)	(-10)°C
Heat Generated ($Q_{(gen)}$)	30 W
Temperature Difference ($T_{(outlet)}$– $T_{(inlet)}$)	10°C
Number of Fins (N)	20 fins
Air Velocity (v)	1 m/s
Convection Coefficient (h)	4.562546291 W/m²·°C
Fin Height ($h_{(fin)}$)	0.005 m
Mesh Element Size	0.001 m

Case III –B. Steady State Thermal Analysis for 30fins

From the analysis Figure 16, it is confirmed that the surface temperature remains below 70°C, with a maximum value of 30.22°C. This indicates that the finned heat sink design is suitable for application, providing effective thermal management of electronic components.

Case III –C. Steady State Thermal Analysis for 10 fins

From the analysis Figure 17, it is confirmed that the surface temperature remained below 70°C with a maximum value of 35.684°C. This indicates that the finned heat sink design is suitable for application, providing effective thermal management of electronic components.

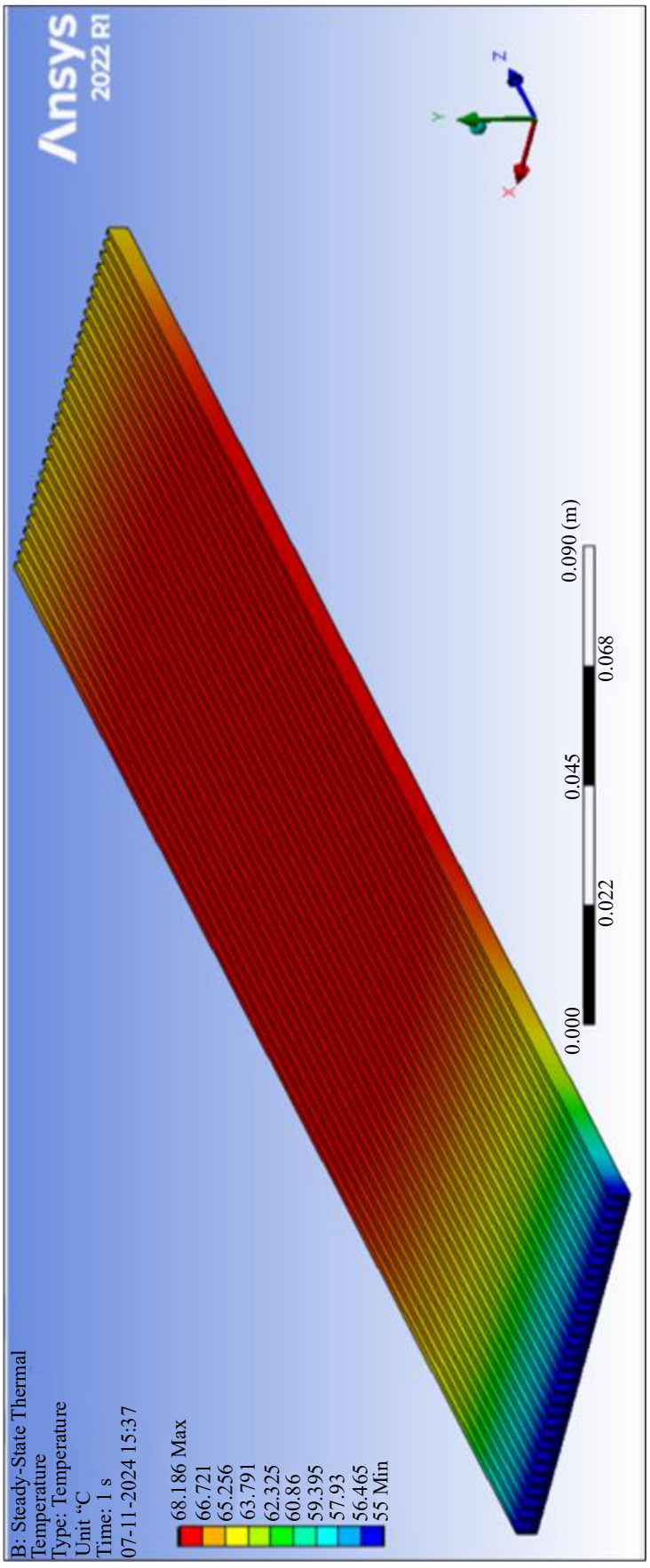

Figure 14. Steady state analysis, temperature variation across surface

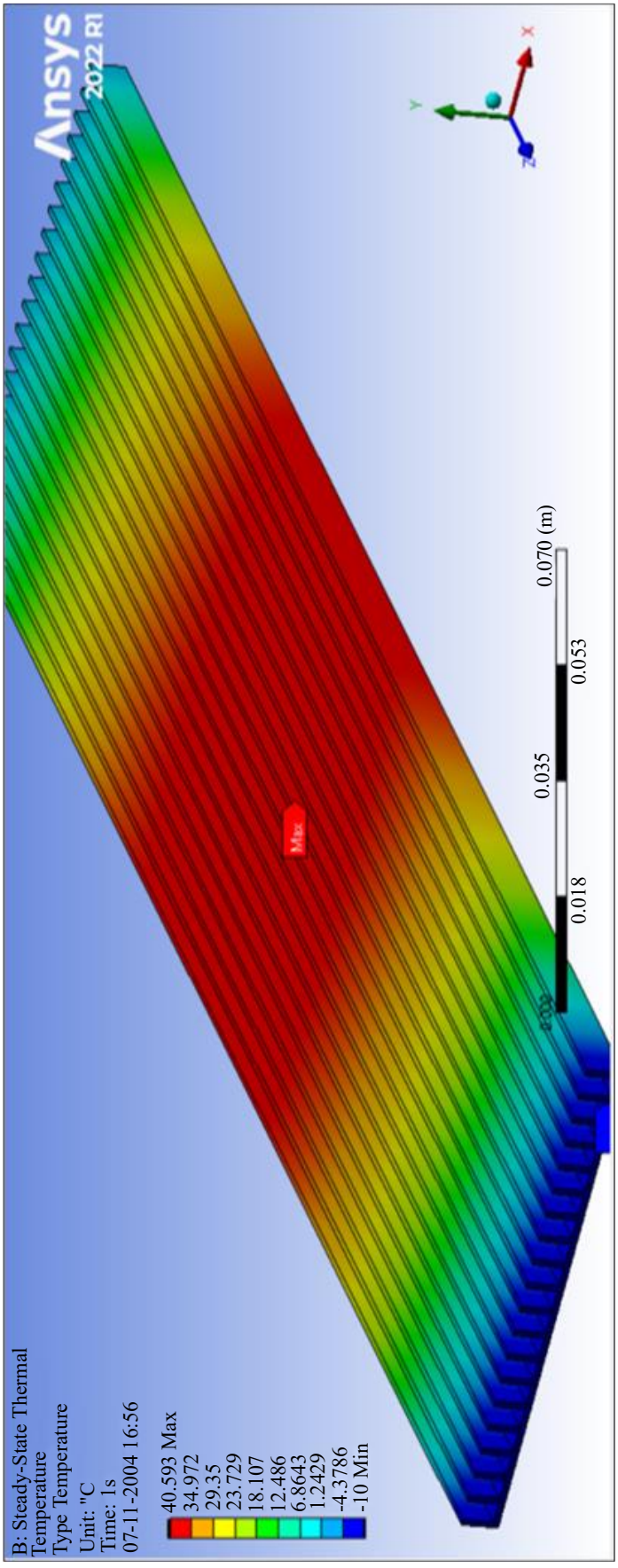

Figure 15. Steady state analysis, temperature variation across surface.

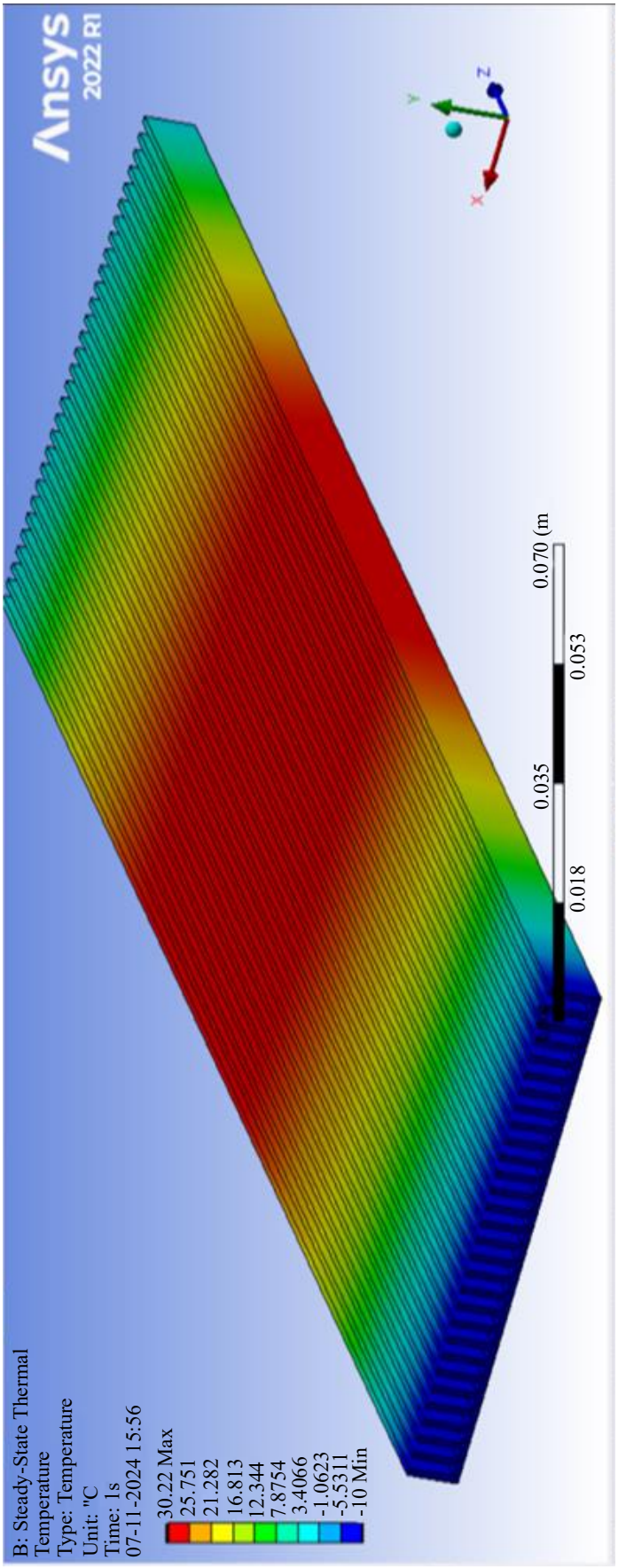

Figure 16. Steady state analysis, temperature variation across surface

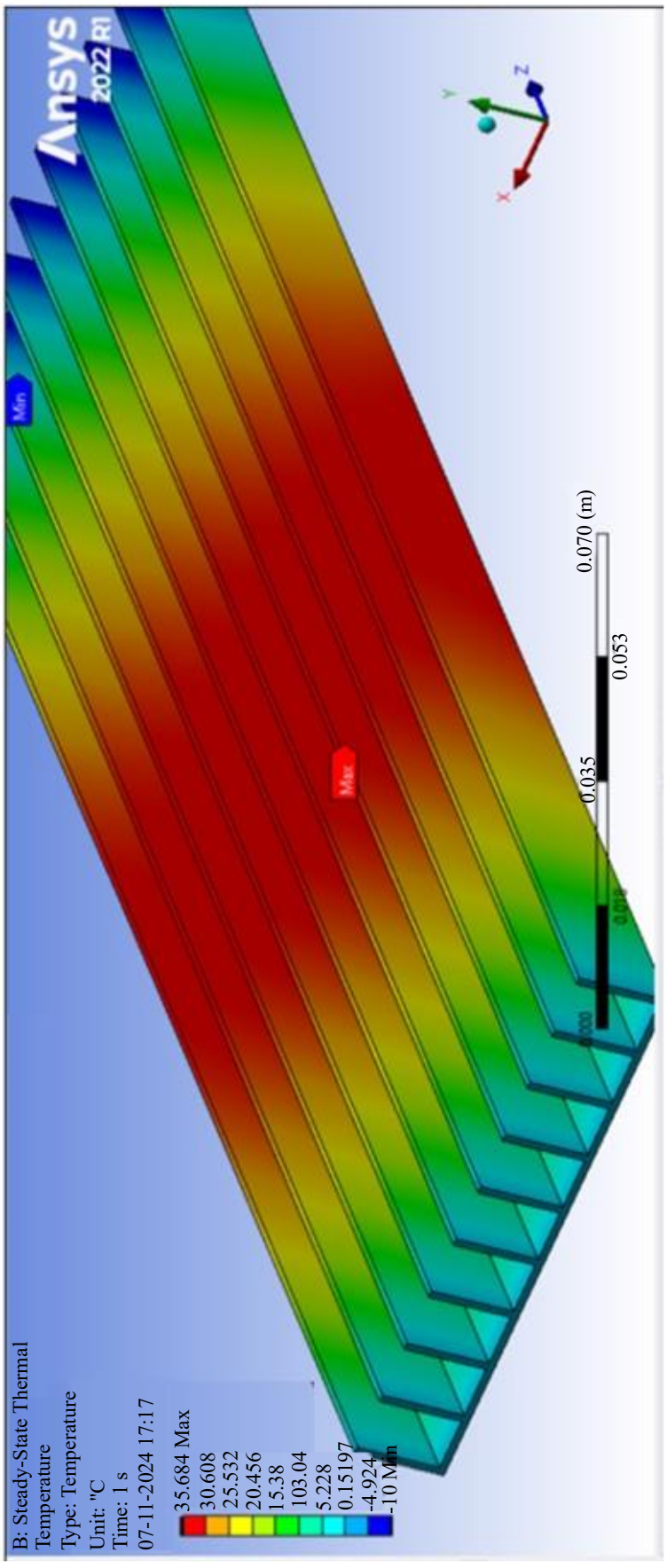

Figure 17. Steady state analysis, temperature variation across surface.

Table 8. Input values of different parameters for CFD analysis.

Parameters	Input Values
Ambient Temperature ($T_{(ambient)}$)	(-10)°C
Heat Generated ($Q_{(gen)}$)	30 W
Temperature Difference ($T_{(outlet)} - T_{(inlet)}$)	10°C
Number of Fins (N)	30 fins
Air Velocity (v)	0.5 m/s
Convection Coefficient (h)	2.62049471 W/m²·°C
Fin Height ($h_{(fin)}$)	0.007 m
Mesh Element Size	0.001m

Table 9. Input values of different parameters for CFD analysis.

Parameters	Input Values
Ambient Temperature ($T_{(ambient)}$)	(-10)°C
Heat Generated ($Q_{(gen)}$)	30 W
Temperature Difference ($T_{(outlet)} - T_{(inlet)}$)	10°C
Number of Fins (N)	30 fins
Air Velocity (v)	1 m/s
Convection Coefficient (h)	4.562546291 W/m²·°C
Fin Height ($h_{(fin)}$)	0.012 m
Mesh Element Size	0.001m

The values in Table 3,4,5,6,7,8 and 9 are considered according to the assumptions made in the paper's objectives and assumptions section.

.

CONCLUSIONS

This research presents a finite element analysis (FEA) of the heat dissipation structure (fins) for an electronic component of a specific dimension (80 × 300 mm) under various controlled conditions using ANSYS software, student version. By creating a 3D model with specified dimensions and conducting an analysis, we validated the calculated values. Although the results from the FEA analysis were closely aligned with the theoretical calculations, minor discrepancies were observed.

These variations can be attributed to the inherent limitations of the numerical methods and computational resources used. Reducing the mesh size to microns can be considered to enhance the accuracy of the simulations.

This leads to a finer discretization of the model, resulting in more precise solutions. Overall, the FEA analysis provided valuable insights into the behavior of the structure, and further refinements in the simulation parameters can improve the correlation between the theoretical and numerical results.

Acknowledgment

The author, S. Menon, wishes to express sincere gratitude to Dr. N. Solanki for the invaluable opportunity to work on this project. The project would not have reached its current level without his expertise, encouragement, and patient mentorship.

Nomenclature

$Q_{(gen)}$: Heat generated by the electronic device
M: Mass flow rate of heat
C_p: Specific heat capacity
T: Temperature
$T_{(outlet)}$: Temperature at Fin Outlet

T_∞: Ambient temperature
$V_{(flow\ rate)}$: Volume flow rate
$m_{(flow\ rate)}$: Mass flow rate of fluid
R_e: Reynolds number
ρ: Density
U: Free stream velocity
D_h: Hydraulic diameter
μ: Viscosity of fluid
h: Convective heat transfer coefficient
N_u: Nusselts number
k: Thermal conductivity
Pr: Prandtl number
A: Area of the electronic device
T_s: Surface temperature
$T_{j'}$: Estimated junction temperature
T_j: Given junction temperature
T_c: Contact temperature
P: Perimeter of fins cross section
m: Fin parameter
Lc: Corrected length
$Q_{(fin)}$: Heat dissipated by the fins
$Q_{(non\ fin\ area)}$: Heat dissipated by non-fin areas
$Q_{(total)}$: heat dissipated by entire arrangement
PLC: Programmable Logic Controller
HMI: Human Machine Interface
UAV: Unmanned Aerial Vehicle
PDB: Power Distribution Board
RADAR: Radio Detection and Ranging
CFD: Computational Fluid Dynamics
FEA: Finite Element Analysis

REFERENCES

1. Han CW, Jeong SB. Evaluation of the thermal performance with different fin shapes of the air-cooled heat sink for power electronic applications. J Int Counc Electr Eng. 2016;6:17–25. doi: 10.1080/22348972.2015.1115168.
2. Özakin AN, Kaya F. Effect on the exergy of the PVT system of fins added to an air-cooled channel: A study on temperature and air velocity with ANSYS Fluent. Sol Energy. 2019;184:561–9. doi: 10.1016/j.solener.2019.03.100.
3. Majmader FB, Hasan MJ. Thermal enhancement and entropy generation of an air-cooled 3D radiator with modified fin geometry and perforation: A numerical study. Case Stud Therm Eng. 2023;52:103671. doi: 10.1016/j.csite.2023.103671.
4. Lan Z, Feng YH, Liu YW. Study of rectangular fin heat sink performance and prediction based on artificial neural network. Case Stud Therm Eng. 2024;64:105569. doi: 10.1016/j.csite.2024.105569.
5. Shuvo MS, Mahmud MJ, Saha S. Multi-scaling analysis of turbulent boundary layers over an isothermally heated flat plate with zero pressure gradient. Heliyon. 2023;9:e22721. doi: 10.1016/j.heliyon.2023.e22721.
6. Pai Raikar PP, Anand N, Pini M, De Servi C. Concurrent optimization of multiple heat transfer surfaces using adjoint-based optimization with a CAD-based parametrization. Int J Heat Mass Transf. 2025;236:126230. doi: 10.1016/j.ijheatmasstransfer.2024.126230.
7. Xie L, Yuan X, Wang W. Thermal modeling of fan-cooled plate–fin heatsink considering air temperature rise for virtual prototyping of power electronics. IEEE Trans Compon Packag Manuf Technol. 2020;10(11):1829–39. doi: 10.1109/TCPMT.2020.3009156.

8. Zhou J, Li X, Feng J, Xu X, Zhang L, Yu Y. Numerical study of non-uniform cooling heat transfer characteristics of supercritical CO2 in horizontal air-cooled finned tube. Case Stud Therm Eng. 2022;37:102263. doi: 10.1016/j.csite.2022.102263.
9. Zhao Z, Zhu L, Wang Y, Huang Q, Sun Y. Experimental investigation of the performance of an air type photovoltaic thermal collector system with fixed cooling fins. Energy Rep. 2023;9:93–100. doi: 10.1016/j.egyr.2023.02.059.
10. Refai-Ahmed G, Do H, Hadad Y, Rangarajan S, Sammakia BG, Gektin V, et al. Establishing thermal air-cooled limit for high performance electronics devices. In: Proc 22nd Electron Packag Technol Conf (EPTC). IEEE; 2020. p. 347–54. doi: 10.1109/EPTC50525.2020.9315139.
11. Gültekina E. Discharging thermal performance evaluation of a lattice-based battery protection package: An experimental approach. [unpublished/online source not specified].
12. Karwa R. Heat and Mass Transfer. Singapore: Springer Nature; 2020. doi: 10.1007/978-981-15-3988-6.
13. Incropera FP, DeWitt DP, Bergman TL, Lavine AS. Fundamentals of Heat and Mass Transfer. New York: John Wiley & Sons; 1996.
14. Cengel YA. Heat Transfer: A Practical Approach. 6th ed. New York: McGraw-Hill Education; 2020.
15. Holman JP. Heat Transfer. 10th ed. New York: McGraw-Hill Higher Education; 2010.

